Electronic Supplementary Information

Unique Trapping of Paddlewheel Copper(II) Carboxylate by Ligand Bound $\{Cu_2\}$ Fragments for $[Cu_6]$ Assembly

Krishna Chattopadhyay,[a] Bikash Kumar Shaw,[b] Shyamal Kumar Saha,[b] and Debashis Ray*,[a]

[a]Department of Chemistry, Indian Institute of Technology (IIT), Kharagpur 721 302, India

[b]Department of Materials Science, Indian Association for Cultivation of Science (IACS), Kolkata 700 032, India

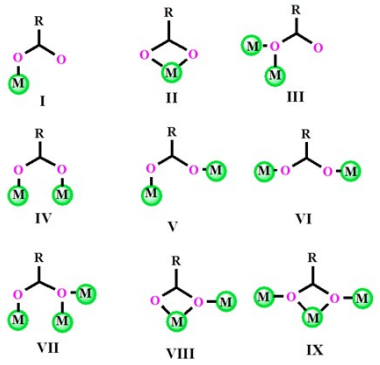

Scheme S1 Different bridging modes of carboxylates.

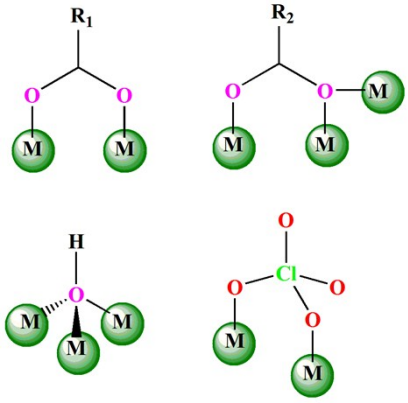

Scheme S2 Bridging carboxylate, hydroxido and perchlorido groups reported in this work.

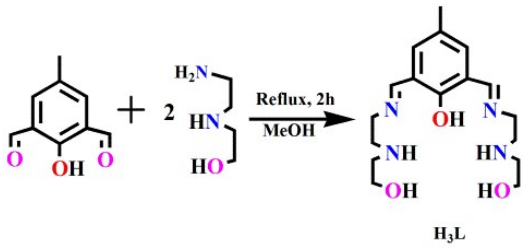

Scheme S3 Synthesis of H_3L.

Table S1 Crystal Data and Structure Refinement Details for Compounds **1-3**[a].

parameters	**1**	**2**	**3**
Formula	$C_{42}H_{70}Cl_4Cu_6N_8O_{33}$	$C_{46}H_{80}Cl_4Cu_6N_8O_{34}$	$C_{66}H_{88}Cl_4Cu_6N_8O_{34}$
F.W. (g mol^{-1})	1738.10	1812.22	2060.48
crystal system	Triclinic	monoclinic	monoclinic
space group	*P*$\bar{1}$	*C2/c*	*C2/c*
Crystal color	Green	Green	Green
Crystal size/mm^3	0.30×0.24×0.15	0.31×0.26×0.15	0.32×0.25×0.17
a/ Å	10.1433(16)	22.6038(9)	30.454(6)
b/ Å	12.7099(19)	12.1267(5)	13.005(3)

c/ Å	14.230(2)	26.1807(11)	24.876(5)
α/ deg	115.462(4)	90.00	90.00
β/ deg	96.643(5)	99.4240(10)	114.482(6)
γ/ deg	104.762(4)	90.00	90.00
V/ Å^3	1547.5(4)	7079.5(5)	8966(3)
Z	1	4	4
D_c/g cm^{-3}	1.865	1.700	1.526
μ (mm^{-1})	2.297	2.013	1.600
F(000)	884	3704	4216
T/K	100	295	295
Total reflns	19239	43821	44447
R(int)	0.0450	0.0762	0.0487
Unique reflns	5892	6924	7803
Observed reflns	4606	4294	5314
Parameters	420	439	525
R_1; wR_2 ($I > 2\sigma(I)$)	0.0464, 0.1213	0.0587, 0.1731	0.0800, 0.2579
GOF (F^2)	1.077	1.020	1.101
Largest diff peak and hole (e Å^{-3})	1.301, -0.983	1.216, -0.471	1.598, −0.789
CCDC No.	1424792	1424793	1424794

[a]$R_1 = \Sigma(||F_o|-|F_c||)/\Sigma|F_o|$. $wR_2 = [\Sigma w(|F_o|-|F_c|)^2/\Sigma w(F_o)^2]^{1/2}$. $w = 0.75/(\sigma^2(F_o) + 0.0010F_o^2)$

Table S2 Selected bond distances (Å) and bond angles (°) in **1-3.**

Bond lengths (Å)					
Complex **1**					
Cu1 − O1	1.954(3)	Cu2 − O1	1.950(3)	Cu3 – O4	2.149(3)
Cu1 – O4	1.955(3)	Cu2 – O4	1.952(3)	Cu3 – O5	1.984(3)
Cu1 – O7	2.586	Cu2 − O10	2.478	Cu3 – O6	1.970(3)
Cu1 – O9	2.527	Cu2 − N3	1.922(4)	Cu3 – O7	1.979(3)
Cu1 − N1	1.924(4)	Cu2 − N4	2.004(4)	Cu3 – O8	1.957(3)
Cu1 − N2	2.007(4)	Cu1---Cu2	2.9808(9)	Cu1---Cu3	3.187
Cu2---Cu3	3.278	Cu3---Cu3*	2.5577(12)		
Complex **2**					
Cu1 − O1	1.956(4)	Cu2 − O1	1.953(4)	Cu3 – O4	2.153(4)
Cu1 – O4	1.963(4)	Cu2 – O4	1.967(4)	Cu3 – O5	1.985(4)
Cu1 – O5	2.514	Cu2 – O6	2.483	Cu3 – O6	1.989(4)

Cu1 – O11	2.679	Cu2 – O12	2.668	Cu3 – O7	1.948(4)
Cu1 − N1	1.923(5)	Cu2 − N3	1.917(5)	Cu3 – O8	1.944(4)
Cu1 − N2	2.005(5)	Cu2 − N4	2.021(5)	Cu1---Cu3	3.239
Cu2---Cu3	3.205	Cu3---Cu3*	2.5401(14)	Cu1---Cu2	2.9980(10)
Complex **3**					
Cu1 − O1	1.930(5)	Cu2 − O1	1.958(6)	Cu3 – O4	2.139(5)
Cu1 – O2	2.436(7)	Cu2 – O4	1.929(5)	Cu3 – O5	1.970(6)
Cu1 – O4	1.964(5)	Cu2 – O10	2.607	Cu3 – O6	1.983(5)
Cu1 − N1	1.929(8)	Cu2 − N3	1.917(8)	Cu3 – O7	1.941(6)
Cu1 − N2	2.008(7)	Cu2 − N4	2.009(9)	Cu3 – O8	1.986(5)
Cu1---Cu2	2.9719(15)	Cu1---Cu3	3.248	Cu2---Cu3	3.3126
Cu3---Cu3*	2.5781(18)				
Bond angles (°)					
Complex **1**					
O1−Cu1−O4	79.78(13)	N2−Cu1−O7	91.42	O4−Cu3−O6	97.61(13)
O1−Cu1−O7	86.7	N2−Cu1−O9	97.05	O4−Cu3−O7	89.65(13)
O1−Cu1−O9	85.11	O1−Cu2−O4	79.92(13)	O4−Cu3−O8	99.84(13)
O1−Cu1−N1	91.99(15)	O1−Cu2−O10	91.52	O5−Cu3−O6	170.60(14)
O1−Cu1−N2	177.55(15)	O1−Cu2−N3	91.26(15)	O5−Cu3−O7	90.37(14)
N1−Cu1−O4	169.00(16)	O1−Cu2−N4	174.62(18)	O5−Cu3−O8	89.38(15)
N1−Cu1−O7	93.9	N3−Cu2−O4	170.49(15)	O6−Cu3−O7	87.25(14)
N1−Cu1−O9	97.97	N3−Cu2−O10	94.50	O6−Cu3−O8	91.48(14)
N1−Cu1−N2	86.56(16)	N3−Cu2−N4	86.72(18)	O7−Cu3−O8	170.51(13)
O4−Cu1−O7	78.45	O4−Cu2−O10	89.34	Cu1−O1−Cu2	99.57(14)
O4−Cu1−O9	88.66	O4−Cu2−N4	101.74(16)	Cu1−O4−Cu2	99.44
O4−Cu1−N2	101. 40(15)	N4−Cu2−O10	93.60	Cu1−O4−Cu3	101.81
O7−Cu1−O9	165.78	O4−Cu3−O5	91.46(13)	Cu1−O7−Cu3	87.51
Cu2−O4−Cu3	106.03				

Complex **2**					
O1−Cu1−O4	80. 07(16)	O1−Cu2−O4	80. 05(16)	O4−Cu3−O5	86.71(16)
O1−Cu1−O5	93.7	O1−Cu2−O6	92.5	O4−Cu3−O6	87.06(16)
O1−Cu1−O11	88.0	O1−Cu2−O12	87.6	O4−Cu3−O7	102.35(17)
O1−Cu1−N1	91.6(2)	O1−Cu2−N3	91.6(2)	O4−Cu3−O8	101.88(16)
O1−Cu1−N2	177.6(2)	O1−Cu2−N4	176.2(2)	O5−Cu3−O6	87. 67(18)
N1−Cu1−O4	171.7(2)	N3−Cu2−O4	171.54(19)	O5−Cu3−O7	170.74(18)
N1−Cu1−O5	103.5	N3−Cu2−O6	100.2	O5−Cu3−O8	91. 43(19)
N1−Cu1−O11	92.4	N3−Cu2−O12	96.8	O6−Cu3−O7	90.87(19)
N1−Cu1−N2	86.1(2)	N3−Cu2−N4	85.7(2)	O6−Cu3−O8	170. 95(18)
O4−Cu1−O5	77.8	O4−Cu2−O6	78.9	O7−Cu3−O8	88.6(2)
O4−Cu1−O11	86. 9	O4−Cu2−N4	102.74(19)	Cu1−O1−Cu2	100.13(18)
O4−Cu1−N2	102.2(2)	O4−Cu2−O12	84.35	Cu1−O4−Cu2	99.43
O5−Cu1−O11	164.0	N4−Cu2−O6	90.66	Cu1−O4−Cu3	103.73
N2−Cu1−O5	86.3	N4−Cu2−O12	90.08	Cu1−O5−Cu3	91.35
N2−Cu1−O11	92.6	O12−Cu2−O6	163.0	Cu2−O4−Cu3	102.07
Cu2−O6−Cu3	90.88				
Complex **3**					
O1−Cu1−O4	79.8(2)	O1−Cu2−O4	80.0(2)	O4−Cu3−O5	91.9(2)
O1−Cu1−O2	106.6(2)	O1−Cu2−O10	84.3	O4−Cu3−O6	99.2(2)
O1−Cu1−N1	92.1(3)	O1−Cu2−N3	91.4(3)	O4−Cu3−O7	98.5(2)
O1−Cu1−N2	175.5(3)	O1−Cu2−N4	176.6(3)	O4−Cu3−O8	90.7(2)
N1−Cu1−O4	165.5(3)	N3−Cu2−O4	166.0(3)	O5−Cu3−O6	88.7(2)
N1−Cu1−O2	106.8(3)	N3−Cu2−O10	95.6	O5−Cu3−O7	169.6(2)
N1−Cu1−N2	85.7(3)	N3−Cu2−N4	86.6(4)	O5−Cu3−O8	87.6(2)
O4−Cu1−O2	87.2(2)	O4−Cu2−O10	94.5	O6−Cu3−O7	88.9(2)
O4−Cu1−N2	101.5(3)	O4−Cu2−N4	102.5(3)	O6−Cu3−O8	169.6(2)
O2−Cu1−N2	77.8(3)	O10−Cu2−N4	93.2	O7−Cu3−O8	93.0(2)

Cu1−O1−Cu2	99.7(3)	Cu1−O4−Cu2	99.5		

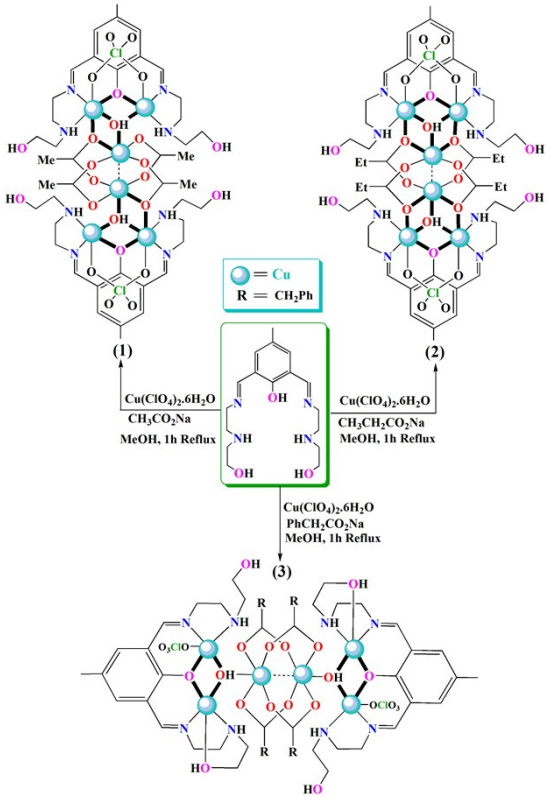

Scheme S4 Synthetic routes for **1-3** (Direct method **A**).

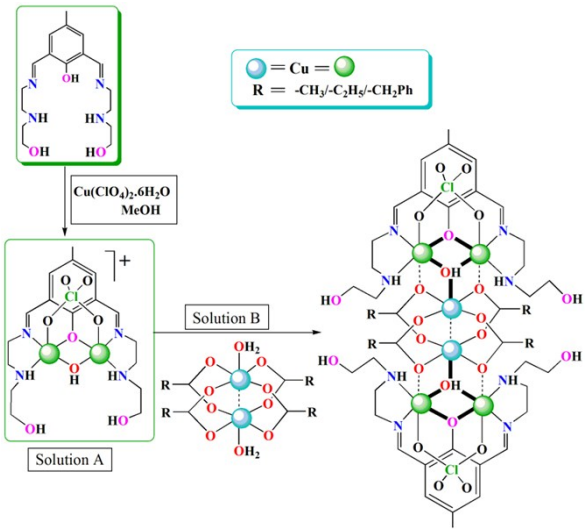

Scheme S5 Alternative path for Complex preparation (Method B).

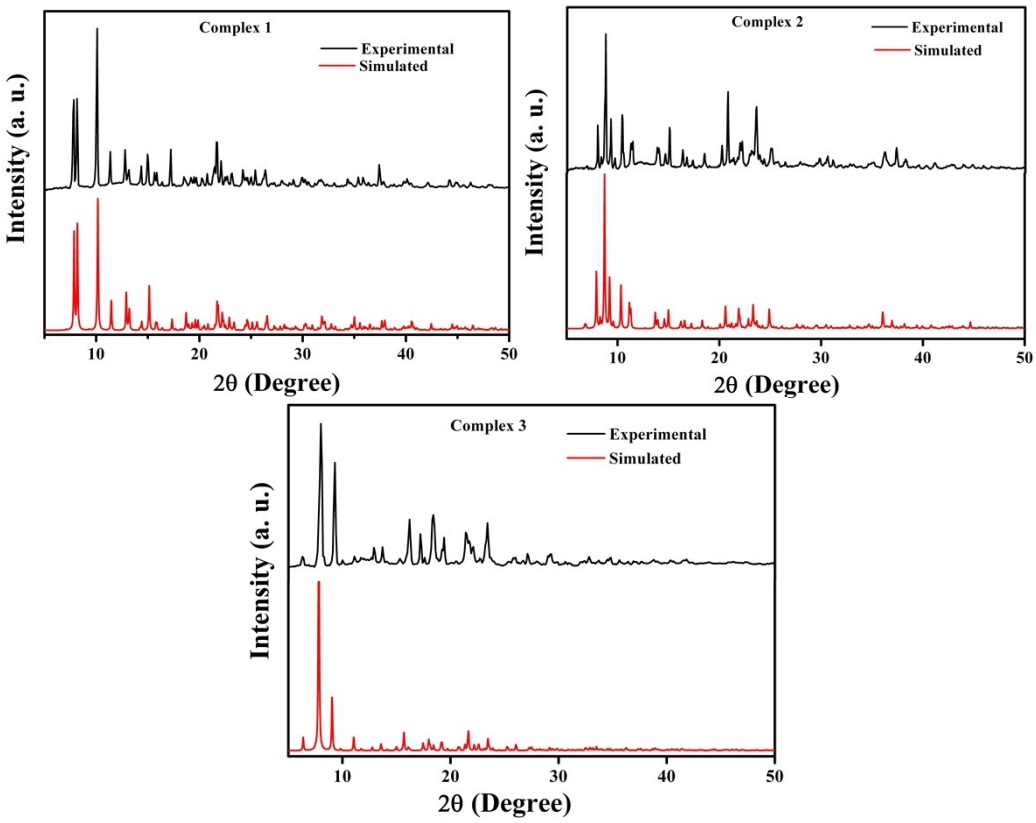

Fig. S1 Matching powder XRD patterns of **1-3** as synthesized (path B) and simulated patterns from the single crystal X-ray structures.

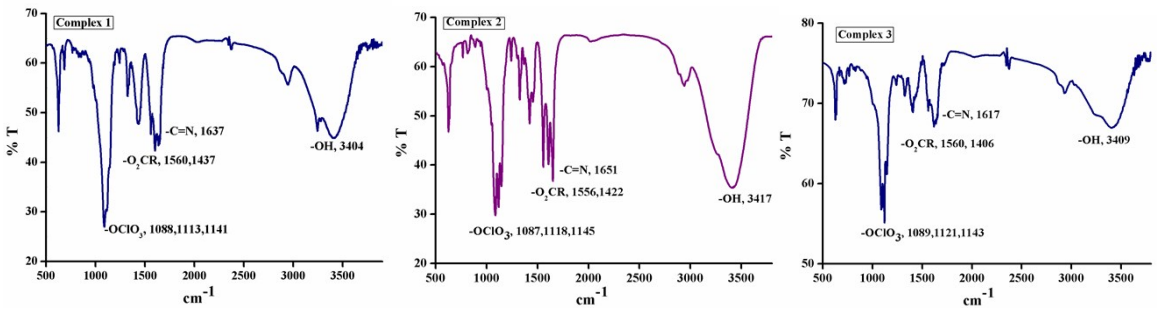

Fig. S2 Comparative FT-IR spectral patterns of **1-3**.

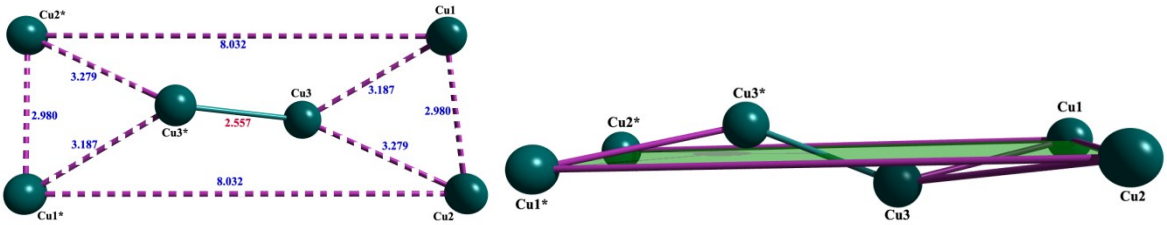

Fig. S3 The Cu_6 parallelogram in **1** showing out of plane positioning of two Cu atoms.

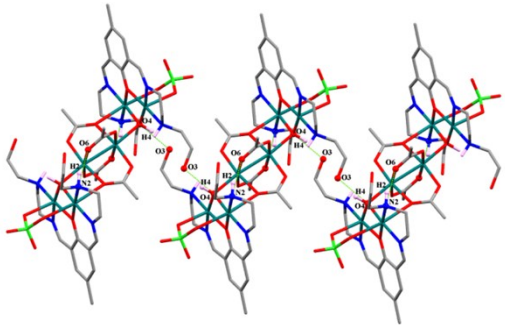

Fig. S4 *Intra*- and *inter*-molecular hydrogen bonding in **1.**

Table S3 Hydrogen bonding parameters of complexes **1**-**3**.

Interactions	D─H (Å)	D···A (Å)	H···A (Å)	D─H···A (º)
Complex **1**				
N2─H2···O2B	0.91	2.775	2.39	105
N2─H2···O6	0.91	3.067	2.25	150
O4─H40···O3	0.98	2.849	1.89	165
O2A─H2A···O16	0.82	3.013	2.34	140
O3─H30···O14	0.82	3.258	2.52	150
N4─H4···O14	0.91	3.242	2.37	160
Complex **2**				
O4─H4···O9	0.98	2.985	2.19	137
O2─H2···O2w	0.82	3.125	2.36	155
N2─H2A···O16B	0.91	3.154	2.27	164
O3A─H3A···N4	0.82	2.859	2.52	106
N4─H4A···O13B	0.91	3.264	2.50	142
N4─H4A···O16A	0.91	3.463	2.56	171
Complex **3**				
N2─H2···O6	0.91	2.963	2.12	153
O4─H4···O3	0.98	2.695	1.82	148
O2─H2A···O9	0.82	2.964	2.31	137
O2─H2A···O10	0.82	3.058	2.50	126
N4─H40···O14	0.91	3.262	2.40	159

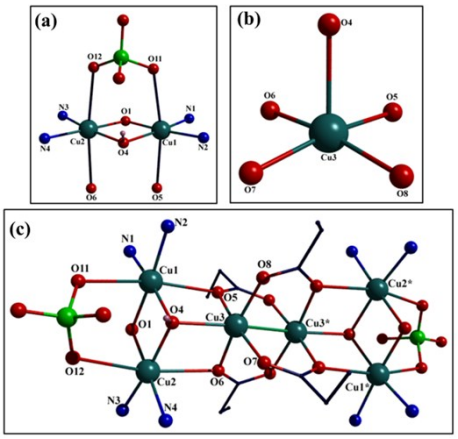

Fig. S5 Core view of **1** showing (a) highly distorted octahedral coordination environment around Cu1 and Cu2, (b) square pyramidal coordination environment around Cu3, and (c) perchlorido group capped hexametallic $\{Cu_6O_{12}\}$ unit.

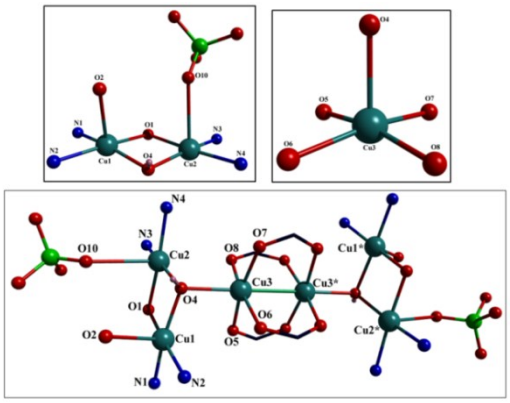

Fig. S6 Core view of **3** showing (a) highly distorted octahedral coordination environment around Cu1 and Cu2, (b) square pyramidal coordination environment around Cu3, and (c) ligand alcohol arm and perchlorido group capped hexametallic $\{Cu_6O_{12}\}$ unit.

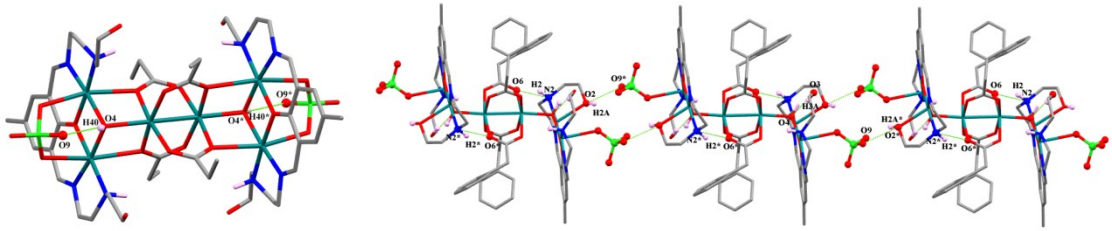

Fig. S7 *Intra*-molecular hydrogen bonding in **2** (left) and*intra*- and *inter*-molecular hydrogen bonding in **3**(right).

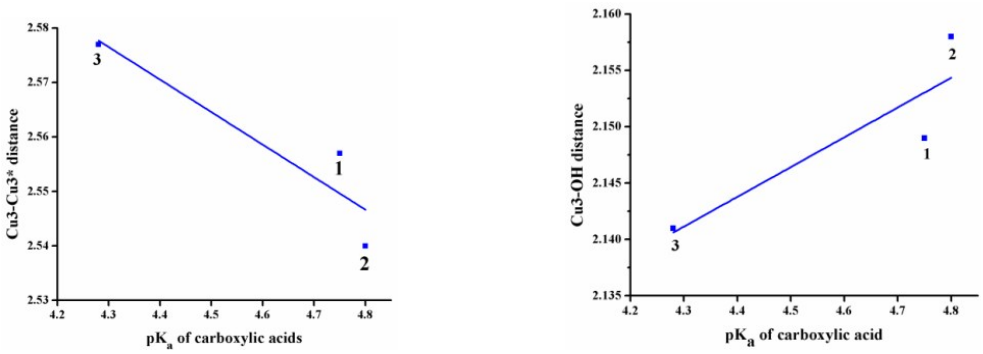

Fig. S8 Variation inCu3···Cu3* and Cu3−OH distances with respect to the *pKa* values of the carboxylic acids in **1**, **2** and **3.**

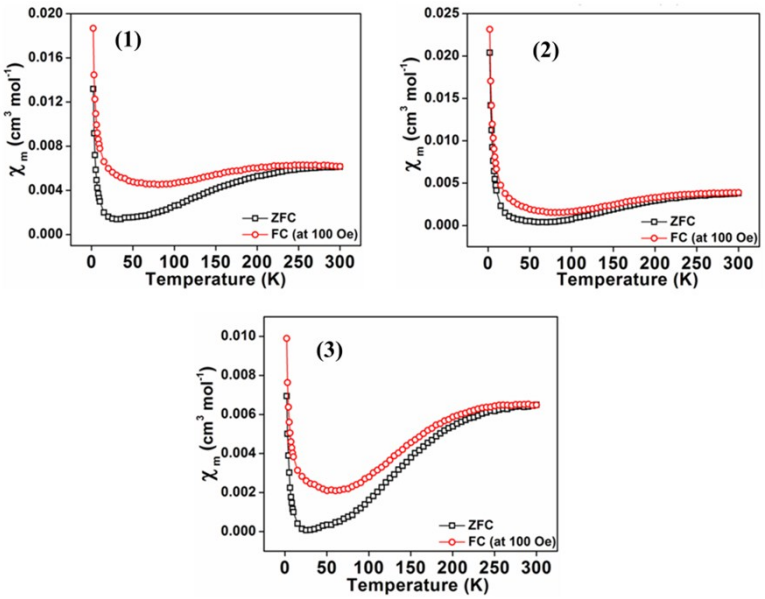

Fig. S9 Changes in molar susceptibility (χ_M) values with temperature for complexes **1**-**3** in zero field cooled-field cooled protocol (ZFC-FC) at 100 Oe magnetic fields.

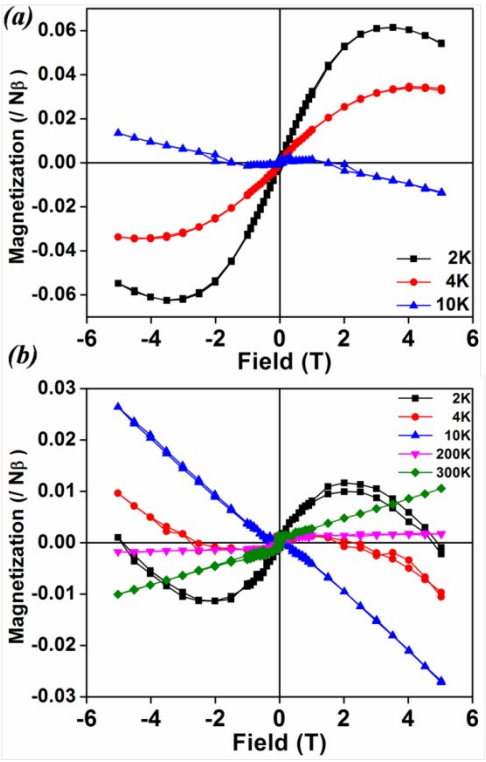

Fig. S10 Variation of magnetization against magnetic field for **1** (a) and **2** (b) at different temperatures.

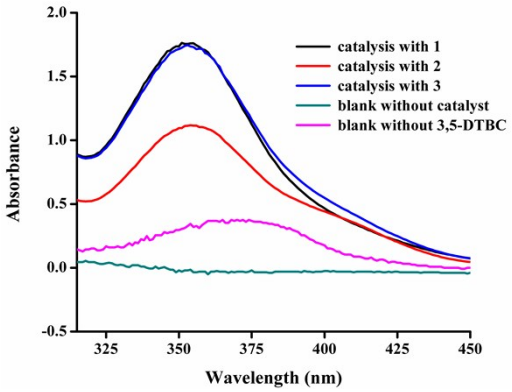

Fig. S11 Absorption spectra of I_3^- confirming the generation of H_2O_2 in the system.

Table S4 Comparison of k_{cat} vaules of complexes **1-3** and other known coppper complexes.

Complex	Solvent	k_{cat} in h^{-1}	Ref
$[Cu_2(L)(\mu\text{-}OH)(H_2O)(ClO_4)_2]$	DMSO	76	32b

$[Cu_2(L1)(\mu\text{-}OAc)](ClO_4)_2\cdot(CH_3)_2CHOH$	MeOH	90	32f
$[\{Cu_2L(\mu_{1,1}\text{-}N_3)(ClO_4)\}_2(\mu_{1,3}\text{-}N_3)_2]$	MeCN	215	32g
$[Cu_2(L2)(\mu\text{-}OAc)](ClO_4)\cdot H_2O\cdot(CH_3)_2CHOH$	MeOH	183	32f
1	MeCN	202	Present work
2	MeCN	387	Present work
3	MeCN	185	Present work

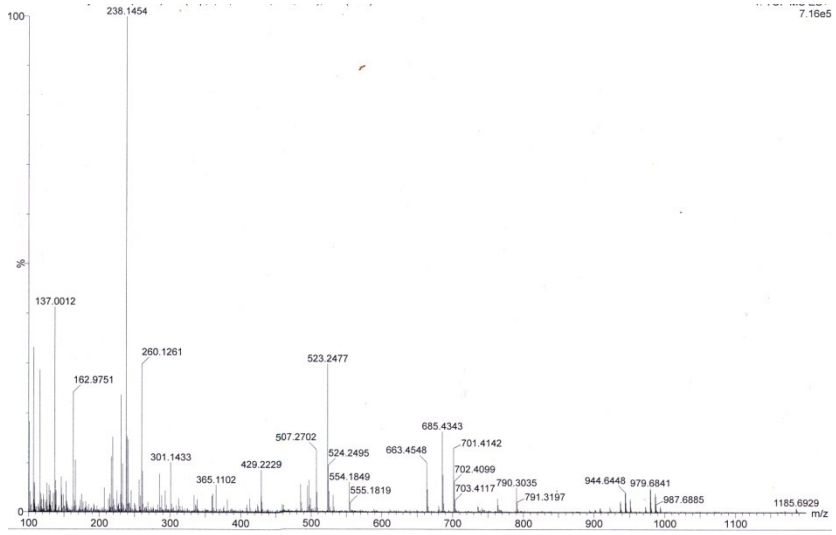

Fig. S12 Electrospray mass spectrum (ESI +ve) of **1** in MeCN.

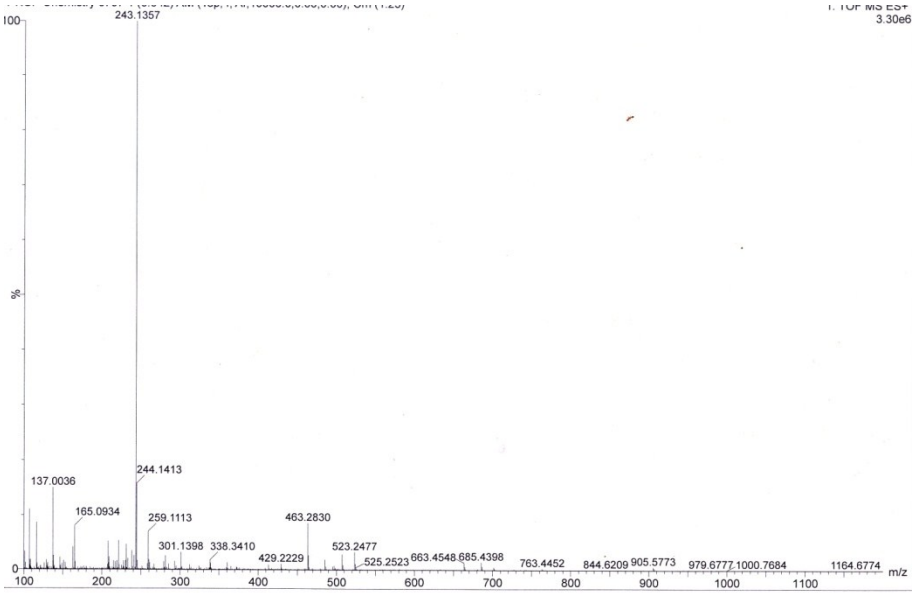

Fig. S13 Electrospray mass spectrum (ESI +ve) of a **1**/3,5-DTBC mixture (1:100) in MeCN and recorded within 5 min of mixing.

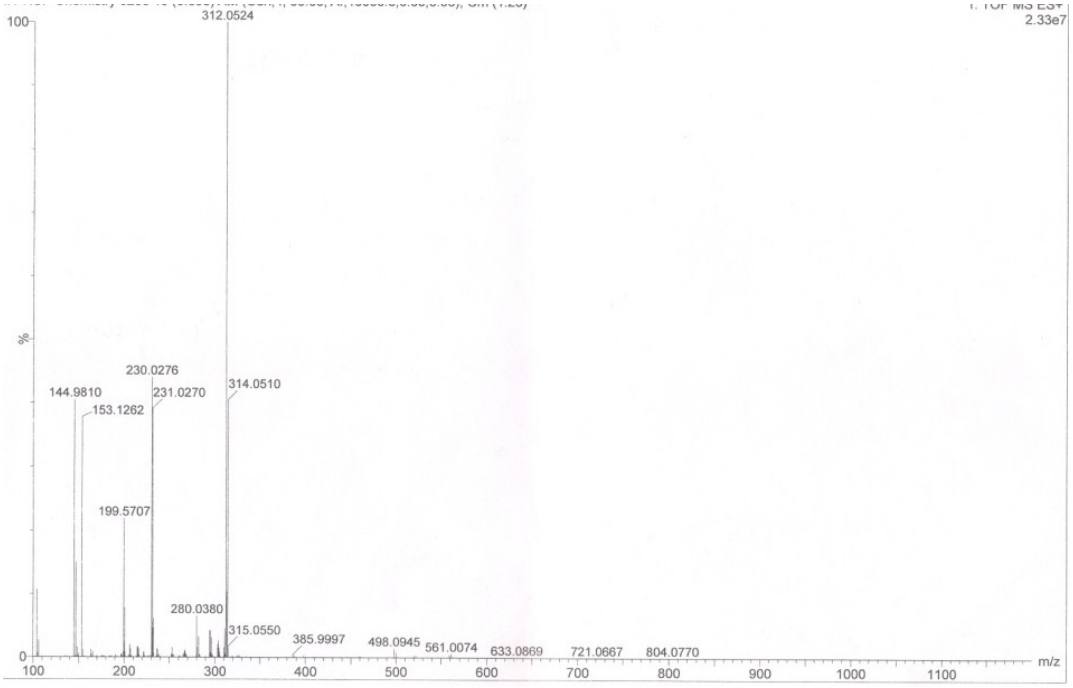

Fig. S14 Electrospray mass spectrum (ESI +ve) of **2** in MeCN.

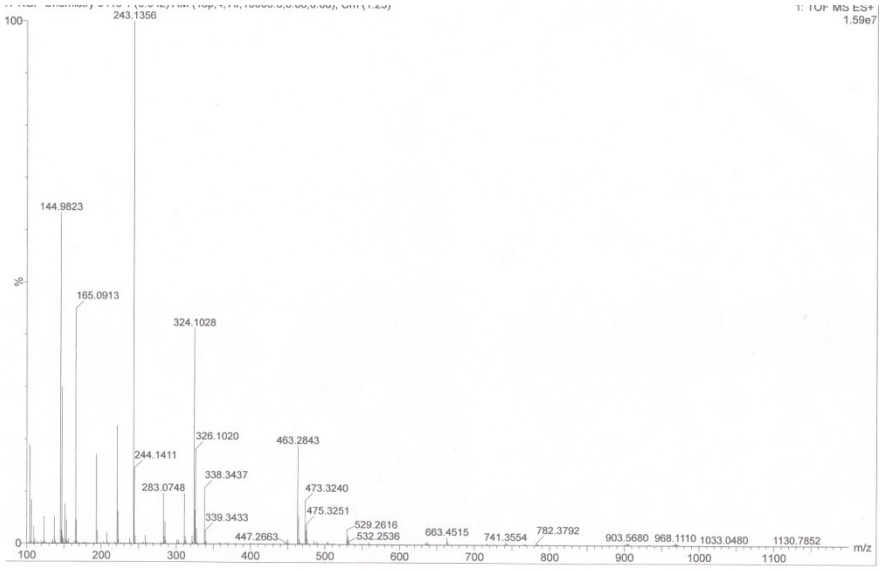

Fig. S15 Electrospray mass spectrum (ESI +ve) of a 1:100 **2**/3,5-DTBC mixture in MeCN and recorded within 5 min of mixing.

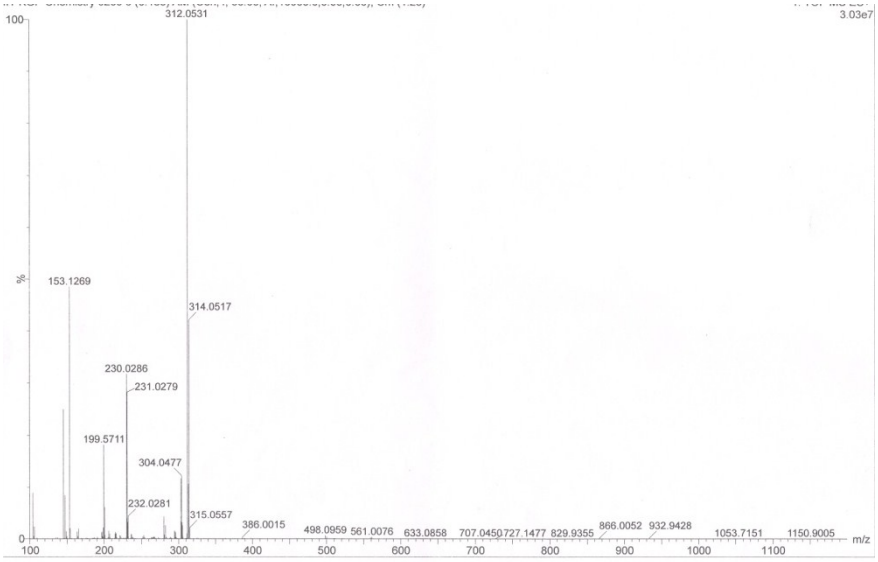

Fig. S16 Electrospray mass spectrum (ESI +ve) of **3** in MeCN.

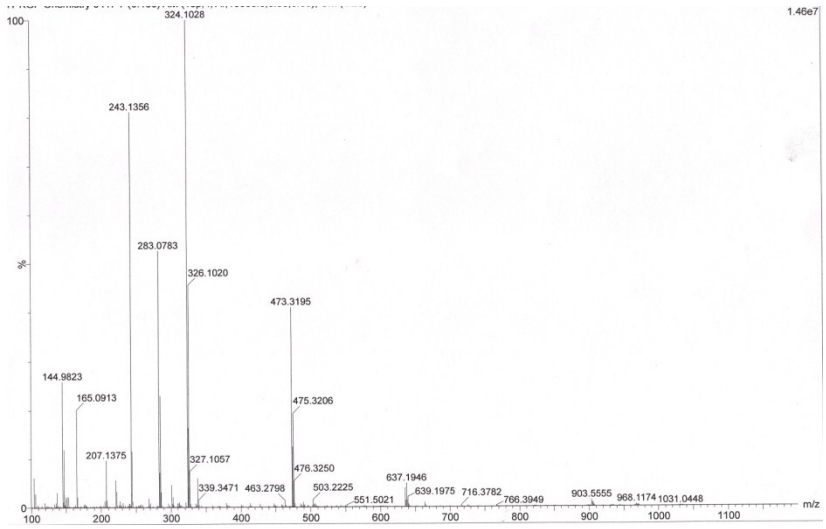

Fig. S17 Electrospray mass spectrum (ESI +ve) of a 1:100 **3**/3,5-DTBC mixture in MeCN and recorded within 5 min of mixing.

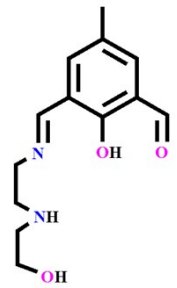

Fig. S18 Partially hydrolysed ligand (HL') in MeCN solution.

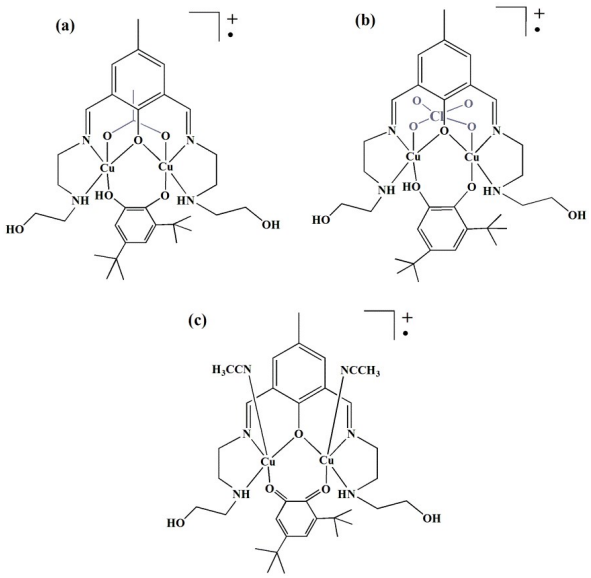

Fig. S19 Possible fragments of complex/catechol aggregates for **1** (a) and **2** (b) and **3**(c).